JOURNAL OF PHYSICAL ORGANIC CHEMISTRY
*J. Phys. Org. Chem.* 2006; **19:** 874–883
Published online 3 November 2006 in Wiley InterScience (www.interscience.wiley.com). DOI: 10.1002/poc.1041

# Structure of D-ribonic acid-dimethyltin(IV) in coordinating solvents: an experimental and DFT $^{119}$Sn NMR study†

**Alessandro Bagno,[1]* Nuccio Bertazzi,[2] Girolamo Casella,[2] Lorenzo Pellerito,[2] Giacomo Saielli[3] and Ivan D. Sciacca[2]**

[1]Dipartimento di Scienze Chimiche, Università degli Studi di Padova, Via Marzolo 1, 35131 Padova, Italy
[2]Dipartimento di Chimica Inorganica e Analitica 'Stanislao Cannizzaro', Viale delle Scienze, Parco d'Orleans II, Università degli Studi di Palermo, Pad. 17, 90128 Palermo, Italy
[3]Istituto per la Tecnologia delle Membrane del CNR, Sezione di Padova, Via Marzolo 1, 35131 Padova, Italy

*Received 2 November 2005; revised 10 January 2006; accepted 12 January 2006*

ABSTRACT: We have investigated a newly synthesized complex of D-ribonic acid with dimethyltin(IV). The structure of the complex in solution has been characterized by means of $^{1}$H, $^{13}$C, and $^{119}$Sn NMR and by DFT calculations. The comparison of experimental and computational results allowed the determination of the stable conformation in solution as well as the detection of a dimerization process. Moreover, evidence is given of active coordination of the metal by the solvent. Copyright © 2006 John Wiley & Sons, Ltd.

KEYWORDS: organotin compounds; ribonic acid; carbohydrate–metal complexes; $^{119}$Sn NMR; DFT calculations

## INTRODUCTION

Diorganotin(IV) derivatives, $R_2SnX_2$ (usually X = Cl, F, OH, COOH, SH; R = alkyl, phenyl) have a wide range of applications in both industrial and basic research. They are used as intermediates in synthesis and their regioselective directing properties are well known,[1,2] especially in synthetic pathways where hydroxy groups are involved.[3] They are also very important in carbohydrate synthetic chemistry.[4] The strong biological activity displayed by organotin(IV) derivatives,[5] including applications in cancer treatment are also well documented.[6–8]

Carbohydrates and their derivatives are also known to have the ability to interact with metal ions present in living organism often acting as chelating agents.[9–11] It is not surprising, therefore, that much interest has been devoted to the study of organotin(IV) complexes with carbohydrates and their derivatives as synthetic intermediates as well as for their biological activity.[4,9–11] When bonded to electronegative atoms, as in carbohydrate complexes, tin(IV) very often presents a coordination higher than four and it is not unusual for diorganotin(IV) derivatives to undergo self-association to give dimers or polymers, or to interact with coordinating solvents. Such structural and dynamical aspects of the chemistry of tin(IV)–carbohydrate complexes need to be carefully considered. To this end, some of us are involved in a thorough study of the chemistry of tin(IV)–carbohydrate systems.[12,13]

$^{119}$Sn NMR, together with the more popular $^{1}$H and $^{13}$C NMR, is a powerful tool to investigate organotin(IV) species in solution: empirical correlation linking the Sn chemical shift to its coordination number and symmetry can be found in the literature, and several reviews about $^{119}$Sn NMR have appeared.[14–17]

Despite this abundance of experimental data, few theoretical studies have been presented in the literature concerning the calculation of $^{119}$Sn NMR parameters. Among these, we mention the work of Nakatsuji *et al.*,[18] who studied the electronic mechanism of the Sn chemical shift on a series of $(CH_3)_{4-n}SnH_n$ and $(CH_3)_{4-n}SnCl_n$ ($n = 0-4$) compounds by *ab initio* methods. More recently, $^{119}$Sn chemical shift were calculated by GIAO-DFT methods by Vivas-Reyes *et al.*,[19] who reported studies of a series of methyltin(IV) compounds at a non-relativistic level; they found a good agreement with experimental data except for $(CH_3)_{4-n}SnBr_n$ ($n = 2$, 3) and $(CH_3)_{4-n}SnI_n$ series ($n = 1$, 2, 3) where spin-orbit (SO) relativistic effects are not negligible. In fact, studies carried out at the finite perturbation SCF level, including the SO correction, on a series of $(CH_3)_{4-n}SnX_n$ (X = halogen; $n = 0$–4), showed that the relativistic effect on the shielding constant of tin might be very large.[20] Other tin compounds have

**Correspondence to:* A. Bagno, Dipartimento di Scienze Chimiche, Università degli Studi di Padova, Via Marzolo I, 35131 Padova, Italy. E-mail: alessandro.bagno@unipd.it
*Contract/grant sponsor:* MIUR; *contract/grant number:* CIP 2001053898_002.
*Contract/grant sponsor:* Università di Palermo; *contract/grant number:* ORPA 41443.
†This article is published as part of the special issue *Festschrift for Norma Nudelman.*

Copyright © 2006 John Wiley & Sons, Ltd.

been investigated by Avalle *et al.*, They calculated, at GIAO-DFT level, the chemical shift of organotin(IV) cyanides[21] and tetraorganotin(IV) derivatives.[22] With regard to spin–spin coupling constants, for small molecules like $SnH_4$ and $SnMe_4$ fairly good results were obtained by means of relativistic four-component calculations.[23,24] In other cases, the agreement with experiment was not very good.[25] Lately, we have presented a comprehensive investigation of $^{119}$Sn NMR properties, calculated with DFT and the two-component ZORA relativistic method.[26] In that study we could successfully model the shielding of tin compounds of widely varying structure, including those containing heavy atoms. The modeling of coupling constants appeared to be less accurate: for alkyltin(IV) halides we showed that $J(^{119}Sn, ^{1}H)$ and $J(^{119}Sn, ^{13}C)$ couplings fall, on the whole, on the same correlation line defined by other $^{119}$Sn–halogen couplings. However, individual values defined a fair correlation of their own with a slope of only 0.3. Even though this correlation could conceivably be used to advantage, the relatively bad performance somewhat calls for caution. In any event, relativistic effects were found to be negligible in practice for tin(IV) compounds containing only light atoms, such as those dealt with herein, because of compensation effects in the calculation of the chemical shift from the shielding constants (see Computational Section). To summarize, valid DFT-based methods to calculate $^{119}$Sn chemical shift have been developed. The results compare well with the experimental data obtained in non-coordinating solvents. When coordinating solvents are used, the chemical shift may depend strongly on the solvent and this effect has to be taken into account.

In this work we present the structural characterization, in water and DMSO, of the complex dimethyltin(IV)-D-ribonic acid ($Me_2$SnRibn) by $^{1}$H, $^{13}$C, and $^{119}$Sn NMR measurements and by DFT calculation of the structural and NMR parameters. D-Ribonic acid (RibnA) is the aldonic acid of D-ribose and in water solution an equilibrium is established where the lactone form ($\gamma$-Ribn) is predominant with respect to the hydrolyzed molecule as reported in Figure 1.

$\gamma$-Ribn lactone is extensively used as chiral template in organic synthesis;[27] phosphorylated derivatives have been found to have biological activity[28] and they also have dermatological uses.[29] As we will show, $Me_2$SnRibn in the coordinating solvents water and DMSO is subject to dimerization and to strong interactions with solvent molecules. A combined experimental and computational approach will be used to understand and separate the various effects and to characterize the system.

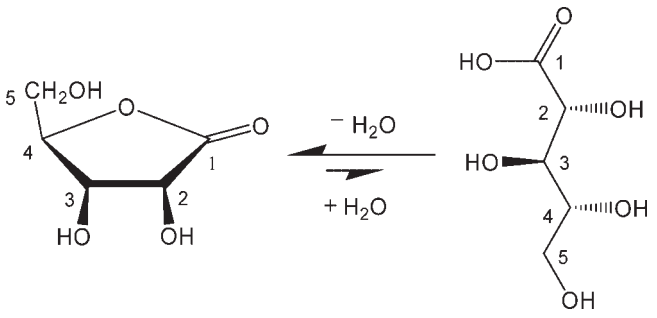


**Figure 1.** Equilibrium between $\gamma$-Ribn and RibnA

## EXPERIMENTAL

### Synthesis of $Me_2$SnRibn

The complex was synthesized from $Me_2SnO$, freshly prepared by hydrolysis of the parent $Me_2SnCl_2$ and D-ribono-1,4-lactone (98% purity, Fluka, Buchs, Switzerland) in a 1:1 molar ratio. D-Ribono-1,4-lactone (296 mg, 2 mmol) was dissolved in 20 ml of water and heated to 80°C for 1 h to allow for the hydrolysis of the lactone ring. The solution was cooled at room temperature and $Me_2SnO$ (328 mg, 2 mmol) was then added. After *ca.* 1 h a colorless solution was formed, which was left to react for 2 days under stirring. The solution was evaporated in a rotary evaporator at 50 °C. The white solid obtained was washed and recrystallized from hot methanol and dried under vacuum in the presence of $P_4O_{10}$. Analytical results for $C_7H_{14}O_6Sn$; Found (calc.): MW = 312.90 (312.89); %C = 26.48 (26.87); %H 4.67 (4.51); %Sn = 37.62 (37.94). The values obtained from the molecular weight measurement by ESI-MS and the elemental analysis were in agreement for a complex with 1:1 ligand:metal stoichiometric ratio where RibnA behaves as a dianionic ligand, conceivably via a deprotonated hydroxyl group.

### NMR measurements

$^{119}$Sn NMR experiments were carried out on a Bruker Avance DRX 300 MHz spectrometer equipped with a 5-mm BBO probe; $^{13}$C and $^{1}$H NMR experiments on Avance DRX 300 and on Avance DMX 600 MHz spectrometers, equipped with a 5-mm BBO *z*-gradient inverse probe and a 5-mm TXI *xyz*-gradient inverse probe, respectively. $^{1}$H signals were assigned by 1D $^{1}$H and 2D-COSY $^{1}$H NMR spectra, while $^{13}$C assignments were performed by 1D $^{13}C\{^{1}H\}$ and 2D-HMQC NMR spectra. $^{1}$H NOESY spectra with different mixing times, ranging from 0.1 to 0.7 s, were acquired to investigate the conformation of the complex and to estimate some proton–proton distances (*vide infra*). $^{119}$Sn chemical shift are referenced to $SnMe_4$ (TMSn, $\delta = 0$). $^{119}$Sn and $^{13}$C spectra were acquired with broadband proton power-gated decoupling.

### Computational methods

In Refs. [19] and [21] the Authors have shown that a triple-zeta basis set is necessary for the calculation of the NMR

Copyright © 2006 John Wiley & Sons, Ltd.

properties of tin. We have used the following methods: geometry optimization was performed using the B3PW91 hybrid functional[30,31] combined with the 6-31G(d,p) basis set for C, H, and O, and the DZVP basis set for Sn. Shielding constants were calculated using the B3LYP [30,32] and B3PW91[30,31] hybrid functionals with IGLO-II[33] for tin and 6-31G(d,p) basis sets for the light atoms. The reference compounds for the nuclei were TMS for $^{13}$C and TMSn for $^{119}$Sn. Their isotropic shielding values ($\sigma_{ref}$) are: 194.88, 191.81 ppm (C) and 2532.60, 2506.92 ppm (Sn) with B3PW91 and B3LYP, respectively. Calculated chemical shifts ($\delta$) were obtained as $\delta = \sigma_{ref} - \sigma$, where $\sigma$ is the shielding of the studied molecule. For all calculations we used the software package Gaussian 98.[34]

## RESULTS AND DISCUSSION

### Experimental NMR studies

In Figure 2 we show the $^{119}$Sn, $^{13}$C, and $^{1}$H NMR spectra of $Me_2$SnRibn in $D_2O$ at room temperature. The $^{119}$Sn{$^{1}$H} spectrum shows two quite broad peaks centered at −114 ppm (with a linewidth $W_{1/2}$ = 2350 Hz) and at −215 ppm ($W_{1/2}$ = 670 Hz).

The signal at −114 ppm falls in the characteristic range of pentacoordinated tin, while the one at −215 ppm falls in a range which is borderline between penta- and hexacoordination in similar diorganotin(IV)–carbohydrate systems.[4,12] The peak at −114 ppm is very close to the one observed for the analogous complex between the dimethyltin(IV) moiety and D-galacturonic acid in $D_2O$;[13] in that case, an active participation of the solvent to the coordination sphere was invoked to account for the pentacoordination suggested by the chemical shift value. Therefore, also in this case, we assign this signal to a monomeric form of the complex in which tin achieves pentacoordination through the addition of a solvent molecule (Fig. 3).

The peak at −215 ppm deserves further investigation. One possibility might be hexacoordinated tin where two solvent molecules have been added to the coordination sphere, but the similarity with analogous systems involving dialkyltin(IV) moieties and simple carbohydrates[4] indicates the possibility of a dimeric form. Thus we suggest that both a monomeric and a dimeric species (Fig. 3) are present and are involved in an exchange equilibrium, also in consideration of the large linewidth of the signals. This hypothesis will be supported by the following discussion of the $^{1}$H and $^{13}$C spectra and by the comparison with the results of DFT calculations (see below). The $^{1}$H and $^{13}$C chemical shifts of $\gamma$-Ribn, RibnA, and $Me_2$SnRibn in 0.1 M $D_2O$ are reported in Tables 1 and 2.

The $^{13}$C{$^{1}$H} spectrum of the complex at room temperature shows a small variation of the carbon resonances, compared to the signals of the free ligand (Table 1) but a significant broadening of the C(3) and C(4) signals (Fig. 2, middle). The C(1) and the methyl carbon resonances of the dimethyltin(IV) moiety are also quite broad. The same considerations apply to the $^{1}$H NMR spectrum of the complex compared to the free ligand: a marked broadening of the H(3) doublet, and a noticeable broadening of the methyl protons resonances occur (Fig. 2, bottom). These observations are in agreement

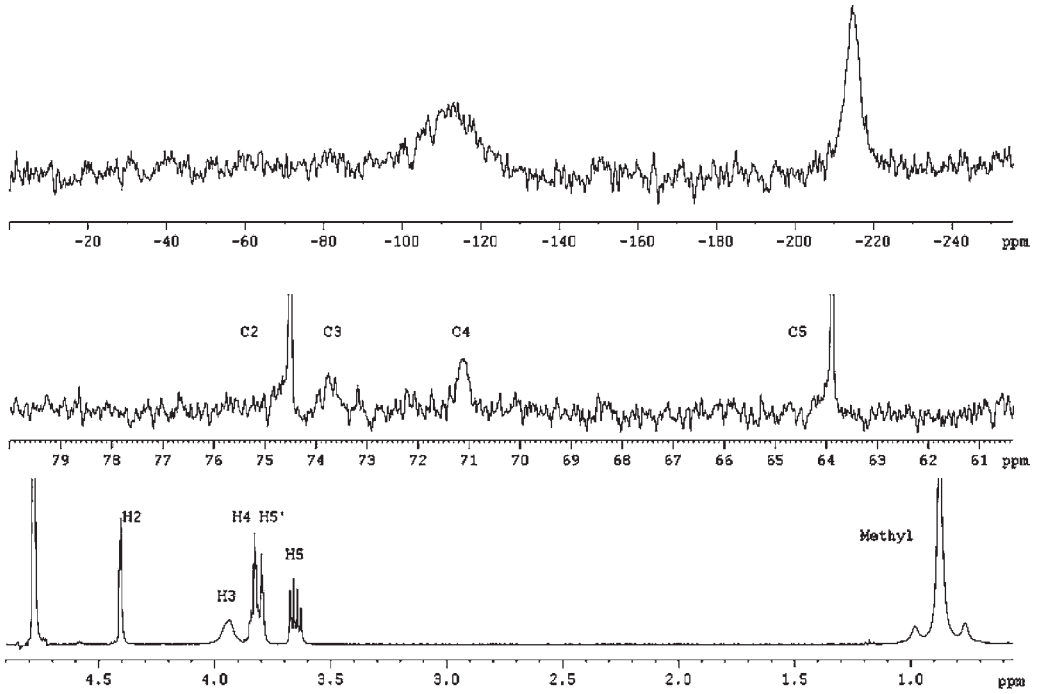


**Figure 2.** Top to bottom: $^{119}$Sn, $^{13}$C (C2–C5 region), $^{1}$H NMR spectra of $Me_2$SnRibn in $D_2O$. Spectra recorded on a 300-MHz instrument (7.05 T)

Copyright © 2006 John Wiley & Sons, Ltd.

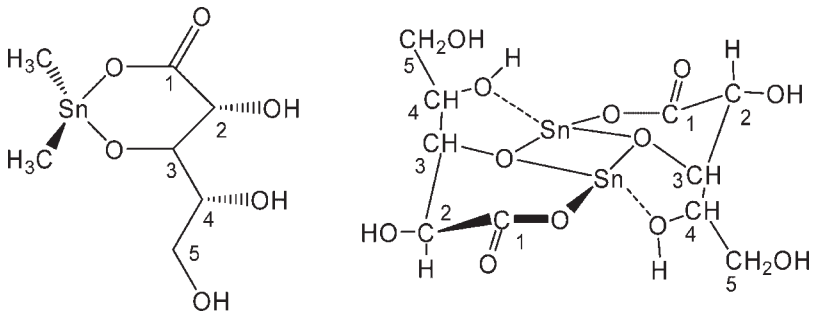

**Figure 3.** Proposed coordination modes for $Me_2SnRibnA$ in monomeric (left) and dimeric (right) $Me_2SnRibn$. For clarity, methyl groups on tin in the dimer are not shown

with a coordination mode of the ligand as a dianionic-chelating agent where the deprotonated O(3) is the second coordinating site, together with the carboxylate group. This results in the formation of a hexa-atomic ring involving the tin atom (Fig. 3).

Qualitatively, a similar behavior is observed in DMSO at room temperature (Fig. 4). Again we observe two resonances in the $^{119}Sn\{^1H\}$ spectrum, at $-100$ ($W_{1/2} = 650$ Hz) and $-206$ ppm ($W_{1/2} = 430$ Hz). The shift to lower frequencies of the tin chemical shift in DMSO compared to water was already observed in analogous systems.[13] A significant broadening, to a greater extent than in water, is observed again for C3 and C4 in the $^{13}C$ spectrum, as well as for the methyl signals in the $^{13}C$ and $^1H$ spectra.

Further information on the conformation of the complex can be obtained from the analysis of proton coupling constants. In the $^1H$ spectrum in $D_2O$ the signal of the methyl groups shows the satellites due to $^2J(^{117,119}Sn, ^1H)$. These satellites are rather broad, so we could only estimate an approximate value of $87 \pm 3$ Hz. This was used in the Lockhart–Manders equation[35] to obtain a value for the C—Sn—C angle of *ca.* $141 \pm 5^\circ$, which suggests a skewed octahedral geometry around tin.

In order to establish the conformation of the ring we estimated the $^3J_{H2,H3}$ value by the Haasnoot–Altona equation,[36] an improved version of the Karplus equation[37,38] in which the electronegativity of the substituents is taken into account. The set of electronegativity values derived by Huggins[39] were used by the Authors.[36] We have parameterized the Haasnoot–Altona equation only for four $\alpha$-substituents since the parameter for tin, a $\beta$-substituent with respect to C3, is not known. From the experimental $^3J_{H2,H3}$ value (2.6 Hz), we estimate two possible H2—C2—C3—H3 dihedral angles in the 0–180° range: 54° and 164°. These values are in agreement with $^3S_2$ and $^2S_3$ conformations, respectively, shown in Figure 5.

The $^1H$ NOESY spectrum in $D_2O$ shows the expected spatial connections between RibnA chain protons. The

**Table 1.** $^1H$ NMR resonances of $Me_2SnRibn$ in $D_2O$ and DMSO-$d_6$

| | | H2 | H3 | H4 | H5 | H5′ | $CH_3$ | $^3J_{2,3}$ | $^3J_{3,4}$ | $^3J_{4,5}$ | $^3J_{4,5'}$ | $^3J_{5,5'}$ |
|---|---|---|---|---|---|---|---|---|---|---|---|---|
| $D_2O$, pH 3.1 | γ-Ribn | 4.76 | 4.54 | 4.60 | 3.90 | 3.81 | b | 5.6 | 7.3 | 3.3 | 4.1 | 13.1 |
| | RibnA[a] | 4.38 | 3.91 | 3.83 | 3.80 | 3.61 | b | | | | | |
| $D_2O$, pH 4.5 | $Me_2SnRibn$ | 4.40 | 3.93 | 3.84 | 3.81 | 3.65 | 0.88 | 2.6 | b | 2.7 | 6.3 | 12.3 |
| | $\Delta\delta$[c] | 0.02 | 0.02 | 0.01 | 0.01 | 0.04 | b | | | | | |
| DMSO-$d_6$ | $Me_2SnRibn$ | 4.06 | 3.74 | 3.57 | 3.55 | 3.42 | 0.64 | | | | | |

[a] The line shape was not well resolved, therefore coupling constants could not be determined.
[b] Signals very broad and/or low in intensity.
[c] Difference between the chemical shift of the complex and the free ligand.

**Table 2.** $^{13}C$ NMR resonances of $Me_2SnRibn$ in $D_2O$ and DMSO-$d_6$

| | | C1 | C2 | C3 | C4 | C5 | $CH_3$ |
|---|---|---|---|---|---|---|---|
| $D_2O$, pH 3.1 | γ-Ribn[a] | 179.90 | 70.40 | 70.93 | 88.16 | 62.00 | b |
| | RibnA | 176.97 | 73.20 | 72.50 | 70.90 | 63.30 | b |
| $D_2O$, pH 4.5 | $Me_2SnRibn$ | 180.32 | 74.48 | 73.52 | 70.98 | 63.91 | 5.68 |
| | $\Delta\delta$[c] | 3.35 | 1.28 | 1.02 | 0.08 | 0.61 | b |
| DMSO-$d_6$[b] | $Me_2SnRibn$ | b | 75.41 | b | b | 64.58 | b |

[a] The γ-Ribn solution was allowed to rest for 1 day at room temperature in order to attain the equilibrium between γ-Ribn and RibnA; the mesaured RibnA: γ-Ribn ratio, obtained from the $^1H$ spectrum, was *ca.* 1:50.
[b] Signals very broad and/or low in intensity.
[c] Difference in chemical shift between the complex and the free ligand.

Copyright © 2006 John Wiley & Sons, Ltd.

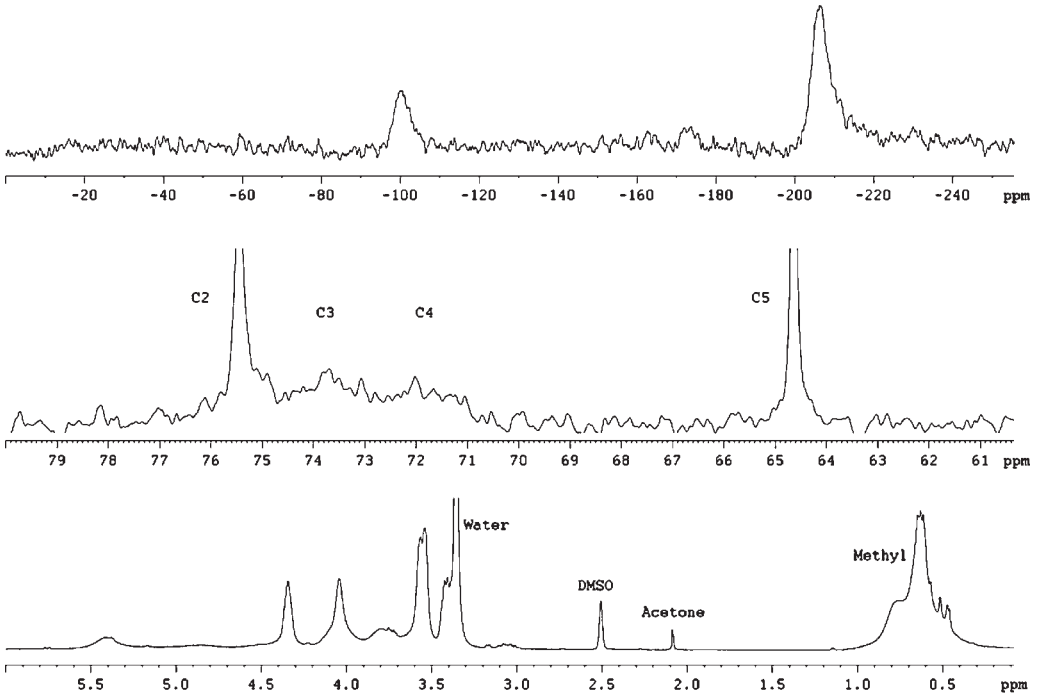


**Figure 4.** Top to bottom: $^{119}$Sn, $^{13}$C (C2–C5 region), $^{1}$H NMR spectra of $Me_2$SnRibn in DMSO. Spectra recorded on a 300-MHz instrument (7.05 T)

methyl groups of $Me_2$Sn(IV) also show connections with H(2), H(3), and H(5) of the ligand. Further $^{1}$H NOESY spectra were carried out at different mixing times (see Experimental Section) to estimate the $CH_3$—H(2) and $CH_3$—H(3) distances to establish the ring conformation: for both distances we obtained a result of *ca*. 3 Å. Such a value agrees with only one of the two possible values of the H(2)–H(3) dihedral angle, that is, 164°. Therefore the six-membered ring possesses a $^{2}S_3$ conformation, where the tin atom lies in the ring plane (Fig. 5). Moreover, the $CH_3$/H(5) cross-peak can be explained considering the dimeric species because the distances between H(5) and the methyl groups fall in a range 2.48–3.30 Å (see Computational Section).

Additional $^{13}$C spectra were acquired at different temperatures and fields (334, 318, and 301 K at 7.05 T, and 318, 301, 278 K at 14.09 T) to qualitatively investigate the exchange dynamics of the system (Table 3, Figs. 6 and 7). The $^{13}$C spectra showed a slight shift towards higher frequencies of all signals upon increasing the temperature.

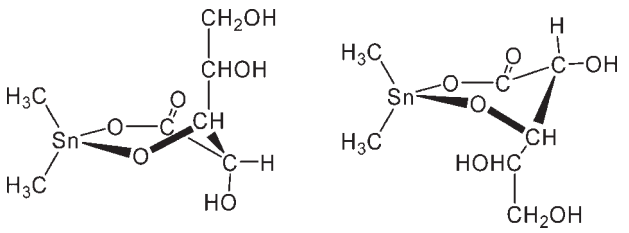


**Figure 5.** $^{3}S_2$ (left) and $^{2}S_3$ (right) conformations for monomeric $Me_2$SnRibn

It is evident, from the dependence of some resonances on temperature and field strength, that C(3), C(4), and H(3) and to a lesser extent H(4), are involved in an exchange process. These results are in agreement with the proposed coordination mode shown in Figure 3, where the oxygen on C(3) is bound to tin. Therefore the same carbon and hydrogen atoms are broadened (Table 3). It is more difficult to explain the similar broadening of carbon in position 4. The conformational energy does not allow the alkyl chain to coil so that O(4) coordinates to tin in the monomer. However, if we consider the dimer this discrepancy is reconciled. In the dimer, the O(4) of one unit can interact easily with the tin atom of the other unit. Therefore, sites 3 and 4 of Ribn are involved in the coordination with tin, so their signals change upon complexation. We note that the $^{2}S_3$ conformation we have proposed does allow the interaction between the hydroxyl OH(4) and the tin atom in the dimer (Fig. 3). Such an interaction would not be possible considering the $^{3}S_2$

**Table 3.** $^{13}$C line widths of $Me_2$SnRibn signals at different fields and temperatures in $D_2O$[a]

| B (T) | T (K) | C1 | C2 | C3 | C4 | C5 | $CH_3$ |
|---|---|---|---|---|---|---|---|
| | 300 | — | 5 | 50 | 18 | 4 | 13 |
| 7.04 | 318 | — | 5 | 9 | 8 | 4 | 56 |
| | 334 | — | 5 | 7 | 7 | 4 | — |
| | 278 | — | 7 | — | — | 18 | — |
| 14.07 | 298 | 96 | 7 | 120 | 60 | 8 | 200 |
| | 318 | — | 5 | 20 | 18 | 4 | 130 |

[a] In Hz with an estimated error of 1 Hz. Where values are missing, the intensity and/or the line width did not allow to get meaningful results.

Copyright © 2006 John Wiley & Sons, Ltd.

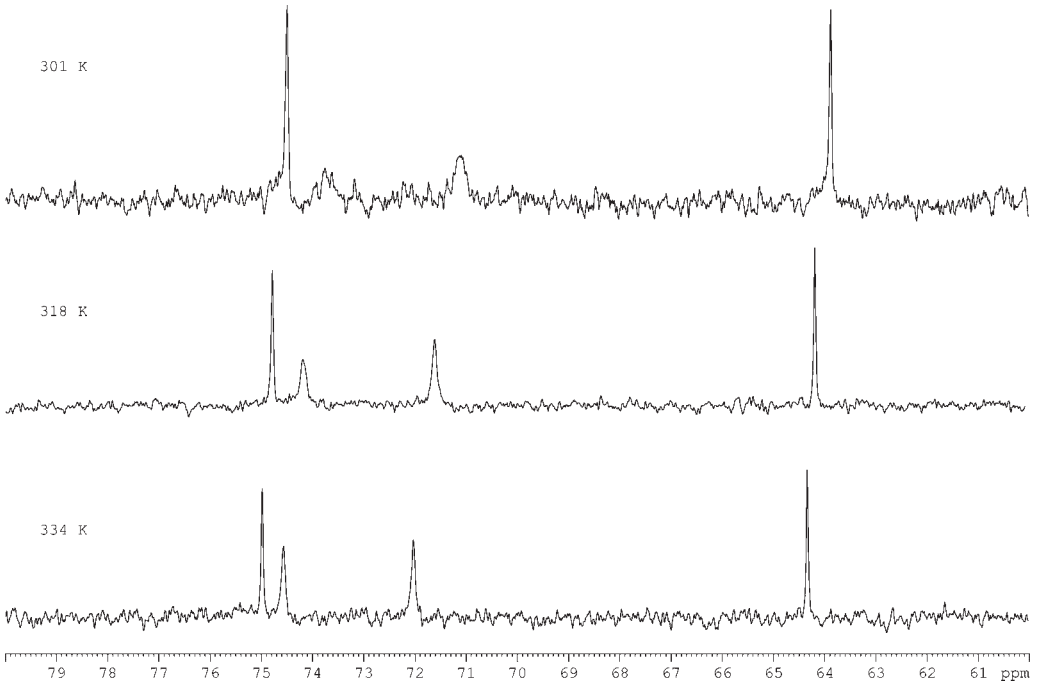


**Figure 6.** $^{13}C$ spectra of $Me_2SnRibn$ in $D_2O$ at the reported temperatures for a field strength of 7.05 T

conformer because of the large separation between the hydroxyl OH(4) of a monomeric moiety in the dimer and the tin atom of the other moiety.

Even though monomer and dimer are clearly subject to an exchange process, we cannot derive quantitative kinetic data from our measurements because solubility problems did not allow us to explore a temperature range where coalescence is reached. However, we note that, for a field of 7.05 T (300 MHz for $^1H$), the resonance frequencies of $^{119}Sn$ and $^{13}C$ are 112 and 75 MHz, respectively. Therefore, the observed separation of about 100 ppm between the two signals in the $^{119}Sn$ spectrum corresponds to a difference of 11 kHz ($10^4$ Hz), far too large for reaching coalescence under chemical exchange; thus, separate (albeit broadened) signals are recorded. In contrast, the $^1H$ and $^{13}C$ resonances of the same two species, assuming that the frozen spectra of the exchanging species are separated by 0.1 ppm for protons

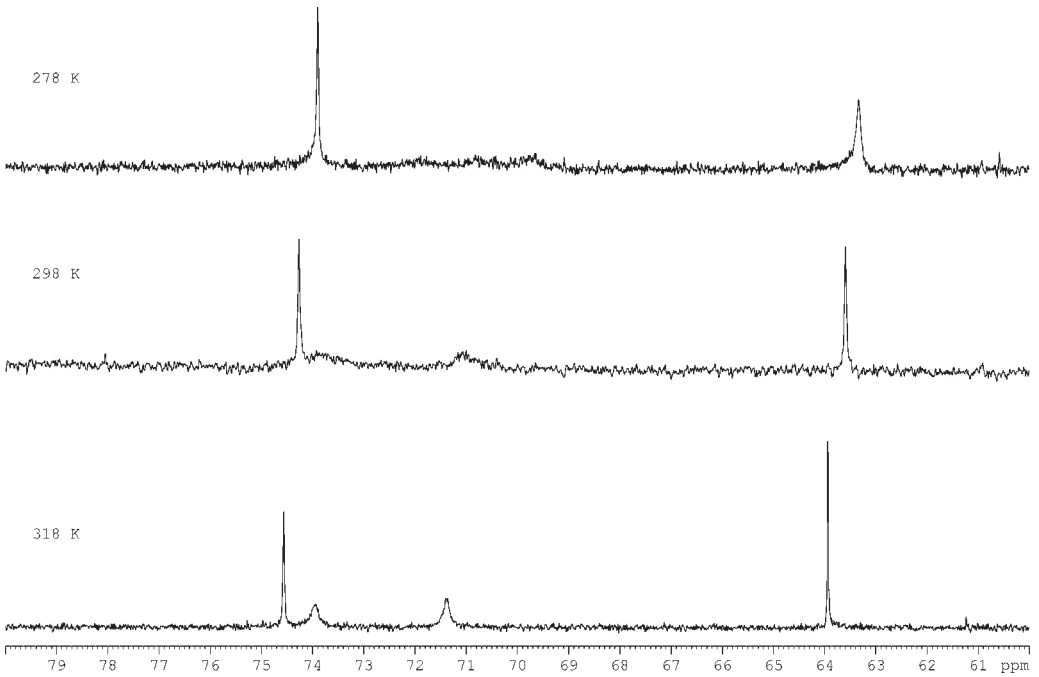


**Figure 7.** $^{13}C$ spectra of $Me_2SnRibn$ in $D_2O$ at the reported temperatures for a field strength of 14.08 T

Copyright © 2006 John Wiley & Sons, Ltd.

and few ppm for carbons (Tables 1 and 2), would be separated by some 30 Hz and 100 Hz, respectively. Since we actually observe just one set of $^{1}H$ and $^{13}C$ signals, although broadened, we conclude that the rate of the monomer–dimer exchange process is larger than *ca.* $10^2\,s^{-1}$.

## DFT calculations

In our computational study we have taken into account the dimerization process and solvent effects by explicitly considering coordinating solvent molecules. Thus, we built three different monomer model structures starting from the $^{2}S_3$ conformation of the ring as already discussed. The three models differ for having none (M0), one (M1), or two (M2) water molecules coordinated to the metal (Fig. 8). We also ran calculations for dimeric structures where the OH(4) hydroxyl group does not interact with tin (D1) or does (D2) (Fig. 9). Moreover, the two tin atoms have been made non-equivalent by adding coordinating water to one of them, as shown in Figure 9. This makes a total of four tin sites, denoted as D1, D1′, D2, and D2′, where the prime indicates the presence of an additional water molecule coordinated to tin. This strategy was chosen to reduce the computational effort, since the calculations for the dimer species were quite demanding.

In Table 4 we report some relevant structural data obtained from the optimized structures of the monomer models together with the relative calculated chemical shift values of $^{119}Sn$.

As reported in Table 4, the 'bite angle' upon the tin atom (RO—Sn—OR′) is constant in the three monomeric models and therefore does not depend on the tin coordination environment. In contrast, the C—Sn—C angle formed with the methyl groups is strongly dependent on the coordination mode of the metal. The value of the C—Sn—C angle estimated from the observed $^{2}J(^{119}Sn—^{1}H)$ coupling constant by means of the Lockhart equation is in agreement with the value of the angle in the model M2 (Table 4); this result suggests a hexacoordinated tin for the monomeric species. On the other hand, the calculated $^{119}Sn$ chemical shift values for M0, M1, and M2, differing in the tin coordination, are in the typical range for a tetra-, penta-, and hexacoordinated rings, respectively,[4,14,16,17] and the experimental $^{119}Sn$ chemical shift calculated is close to the calculated value for the model M1. This apparent contradiction indicates that the solvent molecule in the coordination sphere is exchanged with the bulk solvent on the NMR time scale. One could expect the structural data, obtained indirectly from the value of the proton–tin coupling constant and from the tin chemical shift, to be consistent only in the case that the geometry of the compound is unequivocally determined.

Finally, as already mentioned, the calculated dihedral angle between H(2) and H(3) in the optimized structures was of *ca.* 166°, in good agreement with the value of 164° obtained from the Haasnoot–Altona equation. The calculated distances H(2)—$CH_3$ and H(3)—$CH_3$ obtained from the optimized structures in the $^{2}S_3$ conformation were between 3.0 and 3.6 Å, in agreement with the experimental distances obtained from the NOESY spectra. A structure with a $^{3}S_2$ ring conformation was also optimized for comparison: the resulting H(2)—$CH_3$ distance was *ca.* 5–6 Å and the H(3)—$CH_3$ distance was about 4 Å. These distances are not compatible with the observed NOESY correlation, thus confirming the existence in solution of a preferred conformation of the complex.

In Table 5 we report some relevant structural data and NMR properties obtained from the optimized structures of the dimer models. Also in this case, the RO—Sn—OR′ bite angle upon tin is not dependent on its coordination environment.

For the hexacoordinated tin atoms D1′ and D2 (in the former case the sixth ligand is a water molecule while in the latter one is the hydroxyl group on C4) the calculated C—Sn—C angle is in very good agreement with the experimental data. The calculated $^{119}Sn$ chemical shift for D1′ is also in good agreement with the experimental result, while the calculated value for D2 model is 40–50 ppm lower. As already discussed for the

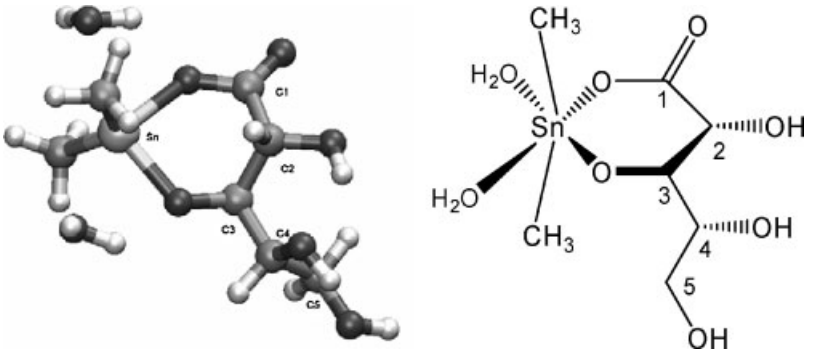


**Figure 8.** Monomer model M2 (see text) having two water molecules coordinated to tin. Left: optimized structure, 3D view. Right: structural formula. Water molecules are stabilized by hydrogen bond interaction with the oxygens on C1 and C3

Copyright © 2006 John Wiley & Sons, Ltd.

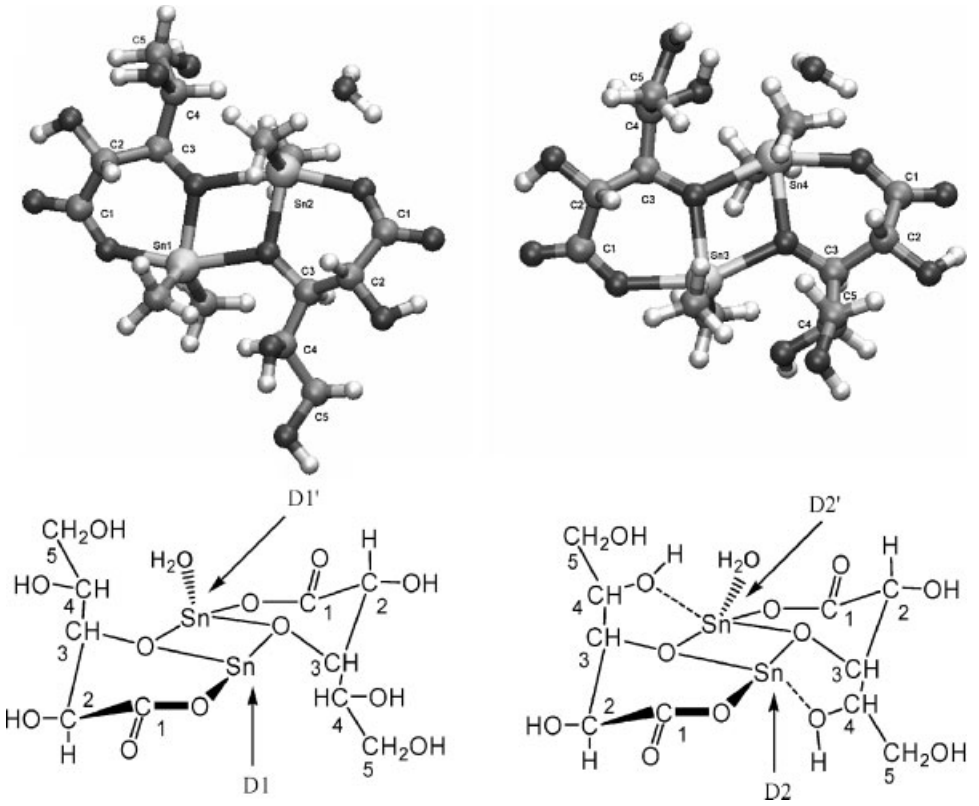


**Figure 9.** Dimer models D1 and D1′ (left) and D2 and D2′ (right). Top: optimized structures, 3D view. Bottom: structural formulas. For clarity, methyl groups on tin are not shown. In both cases the two tin atoms are non-equivalent due to a coordinating water molecule on only one site

**Table 4.** Calculated and experimental structural and NMR data for the monomer models

| | Calc. | | | Exp. |
|---|---|---|---|---|
| Model | M0 | M1 | M2 | |
| No. of water molecules | 0 | 1 | 2 | |
| Coordination[a] | Td | Tbp | Oh | |
| C–Sn–C angle (deg) | 119 | 122 | 135 | $141 \pm 5$[c] |
| O–Sn–O angle (deg)[b] | 96.9 | 96.8 | 96.7 | |
| $\delta(^{119}\text{Sn})$ B3PW91 (ppm) | 80.2 | −102.8 | −188.4 | −114 |
| $\delta(^{119}\text{Sn})$ B3LYP (ppm) | 102.6 | −125.1 | −198.5 | |

[a] Td, tethraedral; Tbp, trigonal bipyramidal; Oh, octhaedral.
[b] Bite angle O(carboxylic)–Sn–O(3).
[c] Bond angle estimated from $^2J(^1\text{H}, ^{119}\text{Sn})$ through the Lockhart equation.[34]

monomeric species, based on these results we cannot exclude the occurrence of coordination modes as in D1′ and D2. In fact, also for the dimer, it is likely that the coordination of a water molecule and the additional coordination from the OH(4) group is a dynamic process on the NMR time scale. What we observe from the NMR experiment is only the average result, both for the chemical shift as well as for the C—Sn—C angle obtained from the proton–tin coupling constant. We note that the distances Sn—OH(4) obtained for the model dimers are in the range 2.48–2.67 Å, thus indicating the possibility of a strong interaction between tin and OH(4). Finally, concerning the observed NOESY correlation between

**Table 5.** Calculated and experimental structural and NMR data for dimer models

| | Calc. | | | | Exp. |
|---|---|---|---|---|---|
| Model | D1 | D1′ | D2 | D2′ | |
| No. $H_2O$/OH(4) group[a] | 0 | 1 | OH(4) | 1/OH(4) | |
| Symmetry[b] | Tbp | Oh | Oh | Hept | |
| C–Sn–C angle (deg) | 131 | 142 | 142 | 165 | $141 \pm 5$[d] |
| O–Sn–O angle (deg)[c] | 86.5 | 87.6 | 84.6 | 85.6 | |
| $\delta(^{119}\text{Sn})$ B3PW91 (ppm) | −174.1 | −220.1 | −253.9 | −416.4 | −215 |
| $\delta(^{119}\text{Sn})$ B3LYP (ppm) | −185.5 | −231.3 | −265.7 | −436.8 | |

[a] The column with 1/OH(4) indicates the coordination of one water molecule and the OH(4) group at the same time upon tin.
[b] Tbp, trigonal bipyramidal; Oh, octahedral; Hept, heptacoordinated.
[c] Bite angle O(carboxylic)–Sn–O(3).
[d] Bond angle estimated from $^2J(^1\text{H}, ^{119}\text{Sn})$ through the Lockhart equation.[34]

Copyright © 2006 John Wiley & Sons, Ltd.

the methyl groups and H(5), we note that, from the optimized structures of the model dimers, the distance between the $CH_3$ protons of one unit and the H(5) of the other unit in the dimer are *ca*. 2.50 Å; this easily explains the presence of cross-peaks in the NOESY spectra arising from the dimer.

In contrast, pentacoordinated tin as in D1 can be excluded because tin could easily bind one further molecule of solvent (like in D1′) while the heptacoordinated tin as in D2′ can be ruled out because of significant deviations of the calculated data from the experimental results (Table 5).

The comparison between the B3PW91 and B3LYP functionals, here and in the case of the monomeric structure, shows that the chemical shift values of tin obtained with the latter functional are systematically shifted towards lower frequencies with respect to the former one. The performance is, however, similarly good in both cases.

## CONCLUSIONS

In this work we have reported on the structural characterization in solution of a new complex between dimethyltin(IV) and D-ribonic acid. We have found that in water and DMSO there is an equilibrium between a monomeric and a dimeric form. This has been clearly deduced from the presence of two signals in the $^{119}$Sn NMR spectrum of the complex. The analyses of the line widths, of some $^{13}$C resonances and of their temperature and field dependence have given some indications concerning the conformational structure of both the monomer and the dimer species. For the dimer the coordinating solvent is competing with the hydroxyl group on C4 in coordinating to the sixth position of a octahedral geometry around tin, while for the monomer it is only the solvent which is involved in a dynamical coordination of tin.

DFT calculations of the geometry and NMR properties of tin support the proposed structures of the monomer and dimer in solution. Moreover, the comparison of the calculated and experimental chemical shifts has been very useful in the assignment of the resonances observed in the $^{119}$Sn spectrum. We also stress the importance of considering exchange processes of solvent molecules in the coordination sphere of tin in order to properly understand the actual coordination of tin(IV) and the experimental NMR results obtained in coordinating solvents.

### Acknowledgements

Calculations were run on an IBM SP4 at the CINECA Supercomputing Center, Bologna, Italy. We thank Dr F. Rastrelli (Universtà di Padova) for help in NMR experiments and Dr A. Giuffrida (Università di Catania) for ESI-MS measurements. Financial support by the Ministero dell'Istruzione, dell'Università e della Ricerca (MIUR, CIP 2001053898_002), by the Università di Palermo (ORPA 41443) is gratefully acknowledged.

## REFERENCES

1. Jousseame B, Pereyre M. In *Chemistry of Tin*, Smith PJ (ed.). Chapman & Hall: London, 1998.
2. Evans CJ. In *Chemistry of Tin*, Smith PJ (ed.). Chapman & Hall: London, 1998.
3. David S, Hanessian S. *Tetrahedron* 1985; **41**: 643–663. DOI: 10.1016/S0040-4020(01)86443-9
4. Grindley TB. *Adv. Carbodr. Chem.* 1998; **53**: 17–142.
5. Arakawa Y. In *Chemistry of Tin*, Smith PJ (ed.). Chapman & Hall: London, 1998.
6. Saxena AK, Huber F. *Coord. Chem. Rev.* 1989; **95**: 109–123. DOI: 10.1016/0010-8545(89)80003-7
7. Tsangaris JM, Williams DR. *Appl. Organomet. Chem*. 1992; **6**: 3–18.
8. Gielen M. *Appl. Organomet. Chem*. 2002; **16**: 481–494. DOI: 10.1002/aoc.331
9. Whitfield DM, Stojkovski S, Sarkar B. *Coord. Chem. Rev.* 1993; **122**: 171–225. DOI: 10.1016/0010-8545(93)80045-7
10. Gyurcsik B, Nagy L. *Coord. Chem. Rev.* 2000; **203**: 81–149. DOI: 10.1016/S0010-8545(99)00183-6
11. Petrou AL. *Coord. Chem. Rev.* 2002; **228**: 153–162.
12. Pellerito L, Nagy L. *Coord. Chem. Rev.* 2002; **224**: 111–150 and references therein. DOI: 10.1016/S0010-8545(01)00399-X
13. Bertazzi N, Bruschetta G, Casella G, Pellerito L, Rotondo E, Scopelliti M. *Appl. Organomet. Chem*. 2003; **17**: 932–939. DOI: 10.1002/aoc.556
14. Smith PJ, Tupčiauskas AP. *Ann. Rep. NMR Spectrosc*. 1978; **8**: 291–370.
15. Hani R, Geanagel RA. *Coord. Chem. Rev.* 1982; **44**: 229–246. DOI: 10.1016/S0010-8545(00)80522-6
16. Wrackmeyer B. *Ann. Rep. NMR Spectrosc*. 1985; **16**: 73–186.
17. Wrackmeyer B. *Ann. Rep. NMR Spectrosc*. 1999; **38**: 203–264.
18. Nakatsuji H, Inoue T, Nakao T. *J. Phys. Chem*. 1992; **96**: 7953–7958. DOI: 10.1021/J100199A025
19. Vivas-Reyes R, De Proft F, Biesemans M, Willem R, Geerlings P. *J. Phys. Chem. A* 2002; **106**: 2753–2759. DOI: 10.1021/JP0145917
20. Kaneko H, Hada M, Nakajima T, Nakatsuji H. *Chem. Phys. Lett*. 1996; **261**: 1–6. DOI: 10.1016/0009-2614(96)00906-2
21. Avalle P, Harris RK, Fischer RD. *Phys. Chem. Chem. Phys*. 2002; **4**: 3558–3561. DOI:10.1039/B202909J
22. Avalle P, Harris RK, Kardakov PB, Wilson PJ. *Phys. Chem. Chem. Phys*. 2002; **4**: 5925–5932. DOI:10.1039/B208435J
23. Kirpekar S, Jensen HJA, Oddershede J. *Theor. Chim. Acta* 1997; **95**: 35–47. DOI: 10.1007/s002140050181
24. Enevoldsen T, Visscher L, Saue T, Jensen HJA, Oddershede J. *J. Chem. Phys*. 2000; **112**: 3493–3498. DOI: 10.1063/1.480504
25. Khandogin J, Ziegler T. *J. Phys. Chem. A* 2000; **104**: 113–120. DOI: 10.1021/JP992571N
26. Bagno A, Casella G, Saielli G. *J. Chem. Theory Comput.* 2006; **2**: 37–46. DOI: 10.1021/ct050173k
27. Bath KL, Chen SY, Joullié MM. *Heterocycles* 1985; **23**: 691–729.
28. Matzanke BF, Böhnke R, Bill E, Trautwein AX, Winkler H. *J. Inorg. Biochem*. 1995; **59**: 111–111.
29. Yu RJ, Van Scott EJ, Aug 1997, U.S. Pat. N. 5,583,156. Yu RJ, Van Scott EJ, Aug 1997, U.S. Pat. N. 5,656,666.
30. Becke AD. *J. Chem. Phys*. 1993; **98**: 5648–5652.
31. Perdew JP, Chevary JA, Vosko SH, Jackson KA, Pederson MR, Singh DJ, Fiolhais C. *Phys. Rev. B* 1992; **46**: 6671–6687.
32. Lee C, Yang W, Parr RG. *Phys. Rev. B* 1988; **37**: 785–789.
33. Kutzelnigg W, Fleischer U, Schindler M. In *NMR Basic Principles and Progress*, Diehl P, Fluck E, Günther H, Kosfeld R, Seelig J (eds). Springer-Verlag: Heidelberg, 1991.
34. Gaussian 98, Revision A.9, Frisch MJ, Trucks GW, Schlegel HB, Scuseria GE, Robb MA, Cheeseman JR, Zakrzewski VG,

Copyright © 2006 John Wiley & Sons, Ltd.

Montgomery JA Jr., Stratmann RE, Burant JC, Dapprich S, Millam JM, Daniels AD, Kudin KN, Strain MC, Farkas O, Tomasi J, Barone V, Cossi M, Cammi R, Mennucci B, Pomelli C, Adamo C, Clifford S, Ochterski J, Petersson GA, Ayala PY, Cui Q, Morokuma K, Malick DK, Rabuck AD, Raghavachari K, Foresman JB, Cioslowski J, Ortiz JV, Baboul AG, Stefanov BB, Liu G, Liashenko A, Piskorz P, Komaromi I, Gomperts R, Martin RL, Fox DJ, Keith T, Al-Laham MA, Peng CY, Nanayakkara A, Challacombe M, Gill PMW, Johnson B, Chen W, Wong MW, Andres JL, Gonzalez C, Head-Gordon M, Replogle ES, Pople JA, Gaussian, Inc., Pittsburgh PA, 1998.

35. Lockhart TP, Manders WF. *Inorg. Chem.* 1986; **25**: 892–895. DOI:10.1021/ic00227a002
36. Haasnoot CAG, dew Leeuw FAAM, Altona C. *Tetrahedron* 1980; **36**: 2783–2792. DOI:10.1016/0040-4020(80)80155-4
37. Karplus M. J. *Phys. Chem.* 1959; **30**: 11–15.
38. Karplus M. *J. Am. Chem. Soc*. 1963; **85**: 2870–2871.
39. Huggins ML. *J. Am. Chem. Soc*. 1953; **75**: 4123–4126.

Copyright © 2006 John Wiley & Sons, Ltd.